

Article

Efficient Utilization of Limonite Nickel Laterite to Prepare Ferronickel by the Selective Reduction Smelting Process

Xin Wang¹, Deqing Zhu^{1,2}, Zhengqi Guo^{1,2,*}, Jian Pan^{1,2}, Tao Lv³, Congcong Yang^{1,2} and Siwei Li¹¹ School of Minerals Processing and Bioengineering, Central South University, Changsha 410083, China² Low-Carbon and Hydrogen Metallurgy Research Center, Central South University, Changsha 410083, China³ Beris Engineering and Research Corporation, Qingdao 265000, China; lvtao@beris.com

* Correspondence: guozqcsu@csu.edu.cn

Abstract: Ferronickel products obtained from the traditional process used to treat limonite nickel laterite usually assay very low-grade Ni, only 3–5% Ni due to the high Fe/Ni ratio of limonite nickel laterite. This paper describes an investigation conducted to upgrade limonite nickel laterites for the preparation of ferronickel by using selective reduction smelting technology. By means of thermodynamic calculations and smelting experiments, the smelting separation mechanism and the behavior of P and S removal in the smelting process, as well as the influence of smelting factors, have been systematically identified. The best production index of ferronickel is obtained under optimized conditions as follows: smelting the pre-reduced lumps at 1525 °C for 45 min with a basicity of 0.60, MgO/SiO₂ ratio of 0.30, and nickel and iron metallization rate of 94.30% and 10.93%, respectively. The resulting ferronickel features a nickel and iron grade of 12.55% and 84.61% and a nickel and iron recovery of 85.65% and 10.87%, respectively. In addition, the content of S and P contained in ferronickel is only 0.11% and 0.0035%, respectively. The ferronickel obtained from the selective reduction smelting process is a fine material for the subsequent stainless steel smelting due to its high Ni grade and low content of impurities.

Keywords: ferronickel; limonite laterite; selective reduction smelting process; parameter optimization; desulfurization; dephosphorization



Citation: Wang, X.; Zhu, D.; Guo, Z.; Pan, J.; Lv, T.; Yang, C.; Li, S. Efficient Utilization of Limonite Nickel Laterite to Prepare Ferronickel by the Selective Reduction Smelting Process. *Sustainability* **2023**, *15*, 7147. <https://doi.org/10.3390/su15097147>

Academic Editor: Francesco Ferella

Received: 22 March 2023

Revised: 20 April 2023

Accepted: 23 April 2023

Published: 25 April 2023



Copyright: © 2023 by the authors. Licensee MDPI, Basel, Switzerland. This article is an open access article distributed under the terms and conditions of the Creative Commons Attribution (CC BY) license (<https://creativecommons.org/licenses/by/4.0/>).

1. Introduction

Annual increases in stainless steel production and the rapid development of batteries, new materials, and other industries have boosted market demand for nickel resources [1–3]. With the continued depletion and dilution of nickel sulfide ore [4,5], the main development direction for the exploitation and utilization of nickel resources has gradually focused on laterite nickel ores [6,7]. China mainly imports laterite from the Philippines, of which 50% is limonite laterite with very low nickel content (about 0.8% Ni), high iron grade (about 40%), and crystal water content [8]. In the context of strong demand for nickel but limited sources of high-quality raw materials, how to utilize low-grade laterite nickel ore economically and effectively has been a major issue for stainless steel enterprises.

Generally, limonite nickel laterite has about 0.8% Ni, 40% Fe, and low Si and Mg content, which is mostly used to produce electrolytic nickel by hydrometallurgical processes [9,10] such as the reduction roasting–ammonia leaching process (RRAL) [11] and high-pressure acid leaching process (HPAL) [12,13]. The recovery rate of nickel in the whole RRAL process is only 75–80% and the recovery rate of cobalt is normally less than 40% while the recovery rate of nickel and cobalt in HPAL process can reach more than 90% [13–16]. However, there are some problems, such as high investment cost and high consumption of sulfuric acid in the HPAL process, resulting in limited application. In China, the sintering blast furnace process, as a mainstream method, has been used to treat limonite nickel laterite to prepare ferronickel. However, there are many problems with the

sintering process due to the intrinsic characteristics of limonite nickel laterite, such as very high solid fuel consumption (over 140 kg/t), low sintering productivity (about 1.0 t/(m²·h), and poor tumble strength (less than 54%) [17–20]. Meanwhile, the subsequent blast furnace smelting process also has many problems, including high coke rate and large amounts of energy consumption. In addition, the ferronickel products obtained from this process usually assay very low-grade Ni, only 3–5% Ni due to the high Fe/Ni ratio of limonite nickel laterite [21,22], which is only used as the raw material for 200 series stainless steel.

Hence, the development of low-energy, low-pollution nickel smelting processes to prepare a superior ferronickel product with high nickel grade has become an essential development direction for limonite nickel laterite [23]. Selective reduction smelting technology has been considered as an effective process to treat nickel laterite to produce ferronickel. It is well known that the Rotary Kiln-Electric Furnace (RKEF) process, as a representative of selective reduction smelting technology, is the most commonly used pyrometallurgical technique for processing nickel laterite ores [24,25]. However, the RKEF process is mainly suited to treating nontronite and saprolite laterite ores to achieve ferronickel with a high Ni content, whereas relatively few studies have reported on this process to upgrade limonitic laterite ore. This is because the high Fe/Ni ratio of limonitic laterite ore results in an un-selective reduction effect and ultimately results in low-grade Ni ferronickel product.

This paper describes an investigation conducted to upgrade limonite nickel laterites for the preparation of ferronickel by selective reduction smelting technology. The nickel grade of ferronickel product is controlled by the metallization ratio of pre-reduced clumps. The effects of temperature, duration, and slag type on smelting behavior are the subjects of this work, which includes a feasibility analysis and experimental studies. In addition, desulfurization and dephosphorization behaviors and relevant mechanisms in smelting process are illustrated in this paper.

2. Methods and Materials

A flowchart of the selective reduction smelting process of laterite nickel ore and a schematic diagram of the smelting furnace are shown in Figure 1.

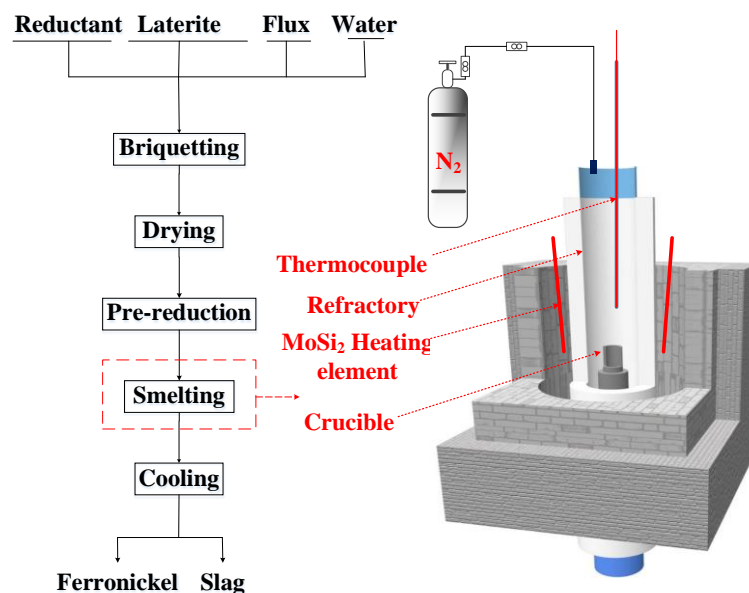


Figure 1. Flowchart of the smelting reduction process of laterite nickel ore and schematic diagram of the smelting furnace.

In this study, by simulating the selective reduction smelting process in the laboratory, low-grade laterite nickel ore was used as raw material to smelt ferronickel. The selective reduction smelting process requires the preparation of pre-reduced lumps; therefore, in

this study, laterite nickel ore was subjected to briquetting, drying, and pre-reduction. The main purpose of this investigation is to study the feasibility of using selective reduction smelting technology to smelt limonite laterite nickel ore and optimize process parameters such as basicity, FeO content, MgO/SiO₂ ratio, smelting temperature, and smelting time.

2.1. Methods

Before the smelting separation experiment, the laterite nickel ore needs to be pre-treated by briquetting, drying, and pre-reduction and the specific process was to first extrude the laterite nickel ore into ellipsoidal lumps with a long axis of 25 mm and a short axis of 10 mm using a counterroll briquetting machine and then complete air-drying on a grate with a size of Φ 200 mm \times 500 mm. Afterward, the pre-reduction process was carried out in a SK-12-13Q vertical resistance furnace to obtain the pre-reduction lump for the smelting separation experiment.

The pre-reduced lump-smelting separation tests were performed in a SG-6-160 high-temperature resistive furnace having the schematic diagram of furnace shown in Figure 1, primarily for the efficient separation of the metal melt and slag. The specific procedure was to first weigh 180 g of the pre-reduced lump and place it in a 150 mL corundum crucible, which was then placed in the furnace at the stated temperature under the protection of an N₂ atmosphere for the smelting separation experiment. Finally, after the smelting experiment was completed and the crucible was sufficiently cooled, the solidified ferronickel and slag were removed from the crucible.

Elements such as Ni, Fe, Si, C, Co, S, and P contained in the ferronickel were determined by using a chemical titration method and the recovery rates of metallic elements were calculated. The calculation formula of the recovery of nickel and iron are as follows:

$$\gamma = \frac{m_0 \times \beta}{m_1 \times \alpha} \times 100 \quad (1)$$

The terms γ , m_0 , m_1 , α and β represent nickel or iron recovery rate, mass of ferronickel product, mass of the pre-reduced lump, iron or nickel grades of pre-reduced lumps, and the iron or nickel grades of ferronickel, respectively.

Furthermore, the phase analysis was adopted for revealing the phase composition of laterite nickel ore by using a series of analytical methods including a Leica DMLP optical microscope and an D8 Advance X-ray diffractometer from the German Bruker Company (Bremen, Germany). For the equilibrium of viscosity, the software program FactSage 7.3 was utilized to calculate the viscosity of slag to satisfy thermodynamics analysis and the smelting temperature of slag was determined based on the hemispherical method.

2.2. Materials

The laterite nickel ore used in this study is from the Philippines and was mixed, dried to about 10% moisture, and then crushed to below 5 mm using a roller crusher. Other raw materials used in this study, including limestone, dolomite, and slaked lime, were all obtained from a Chinese iron and steel enterprise. The chemical compositions of the raw materials and the grain size composition are shown in Tables 1 and 2, respectively. The Ni and Fe grades of laterite ore used in this research are 0.98% and 48.09%, respectively, which is a typical limonite-type laterite nickel ore. In addition, the Co and Cr elements contained in the laterite nickel ore are 0.13% and 2.27% respectively, which also have a certain recovery value. As for the gangue composition of the laterite ore, the Al₂O₃ and SiO₂ contents are as high as 6.32% and 3.97% respectively, while the CaO and MgO contents are only 0.19% and 1.34%, respectively. The size distribution of laterite nickel ore is mainly concentrated between 0.074–3 mm, which is relatively easy for agglomeration.

Table 1. Chemical compositions of raw materials/wt.%.

Minerals	Fe _{total}	Ni	CaO	SiO ₂	MgO	Al ₂ O ₃	Co	Cr	Mn
Laterite	48.09	0.98	0.19	3.97	1.34	6.32	0.13	2.27	1.45
Limestone	0.11	-	0.65	0.65	0.65	0.65	-	-	-
Dolomite	0.56	-	0.75	0.75	0.75	0.75	-	-	-
Slaked lime	0.14	-	1.42	1.42	1.42	1.42	-	-	-
Minerals	K ₂ O	Na ₂ O	Pb	Zn	As	C	P	S	LOI *
Laterite	0.0046	0.040	0.011	0.026	0.0076	0.19	0.32	0.15	12.5
Limestone	-	-	-	-	-	-	0.034	0.0047	42.87
Dolomite	-	-	-	-	-	-	-	-	44.28
Slaked lime	-	-	-	-	-	-	0.065	0.084	30.23

LOI *: Loss on ignition.

Table 2. Size distribution of raw materials/wt.%.

Minerals	Size Fraction/mm					
	>5	3–5	1–3	0.5–1	0.074–0.5	<0.074
Laterite	0.34	4.10	39.57	22.22	29.87	3.90
Limestone	0	4.26	41.56	19.90	30.06	4.22
Dolomite	0	0	0	63.23	34.14	2.63
Slaked lime	0	0	0	0	0	100

In addition, the phase composition of the laterite nickel ore was analyzed using mineral phase microscopy and XRD and the results are present in Figures 2 and 3, respectively. The main mineral compositions of the laterite nickel ore are goethite and feint hematite, followed by a small amount of magnetite and a small amount of gangue dominated by complex aluminosilicate oxides such as nontronite and clinochlore.

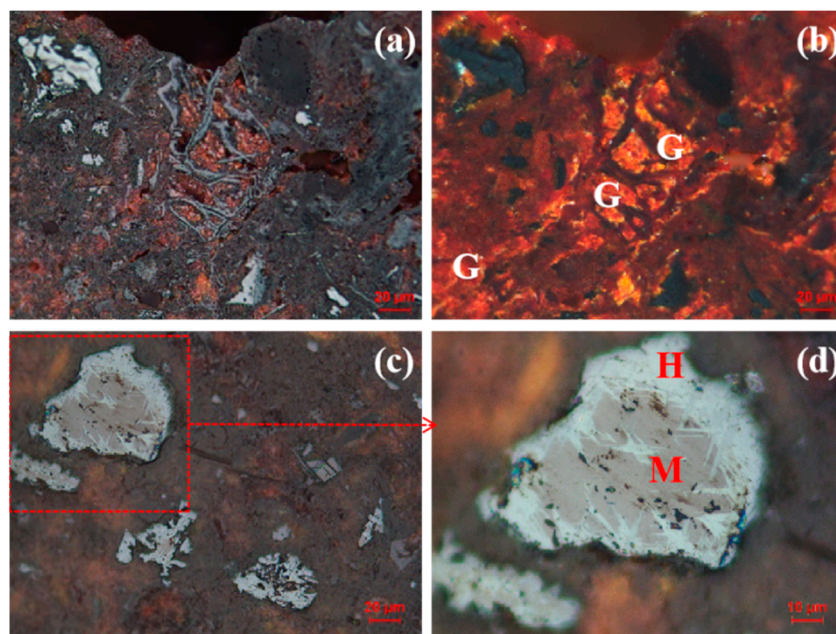


Figure 2. Micro-structure of the laterite nickel ore. (a,c,d) Reflected light; (b) polarized light. G: goethite; H: feint hematite; M: magnetite.

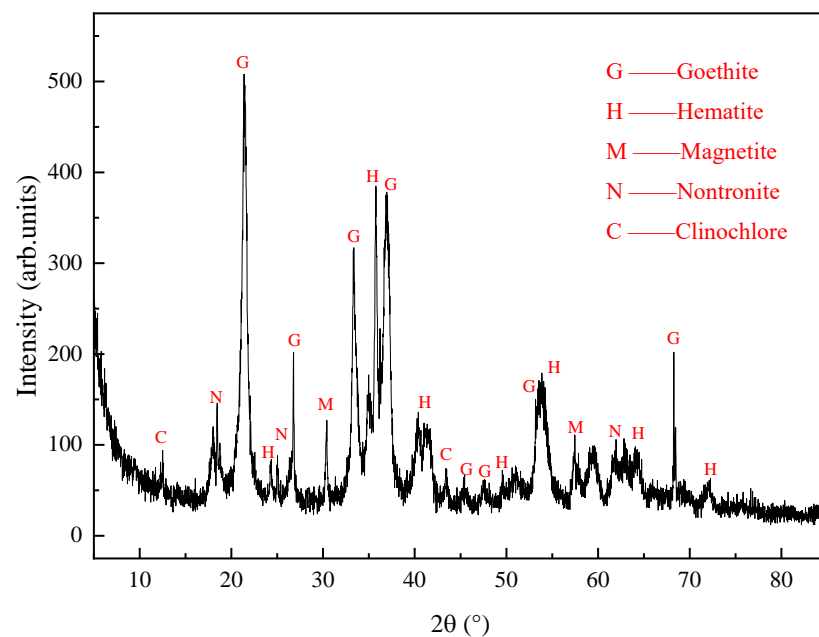


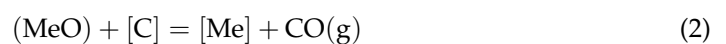
Figure 3. The X-ray diffraction of laterite nickel ore.

3. Results and Discussion

3.1. Thermodynamic Analysis of Smelting Ferronickel

3.1.1. Smelting Separation Mechanism

The phase diagram of $\text{SiO}_2\text{-Al}_2\text{O}_3\text{-CaO-MgO-FeO}$ ($\text{MgO} = 3\%$, $\text{FeO} = 55\%$) is shown in Figure 4. It can be determined that the initial slag phase interval is as shown in the circular region in the figure and the liquidus temperature in this zone is about $1200\text{ }^\circ\text{C}$. The selective reduction smelting process of laterite nickel ore consists primarily of the melting of the reduced lump, separation of the molten slag from the metal melt, and chemical reaction at the liquid–liquid interface. During the smelting process, the soft melting of the burden drops and accumulates in the lower part of the furnace cylinder. At the slag–iron interface, the chemical reaction between the metal element and C can be represented as in Equations (2)–(5) [26–30].



$$K_{\text{Me}} = \frac{\gamma'_{\text{Me}} \cdot \omega[\text{Me}] \cdot P_{\text{CO}}}{a_{(\text{MeO})}} \quad (3)$$

$$\lg K_{\text{Me}} = -\frac{A_{\text{Me}}}{T} + B_{\text{Me}} \quad (4)$$

$$L_{\text{Me}} = \frac{m[\text{Me}]}{m(\text{MeO})} = L_0 \cdot \frac{K_{\text{Me}} \cdot \gamma_{(\text{MeO})}}{P_{\text{CO}}} \quad (5)$$

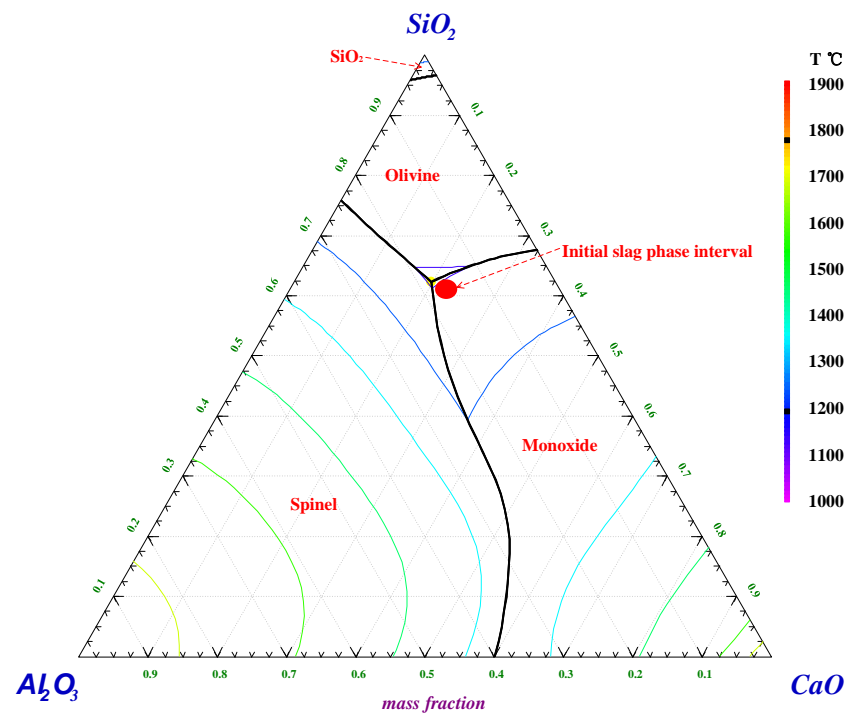


Figure 4. Phase diagram of $\text{SiO}_2\text{-Al}_2\text{O}_3\text{-CaO-MgO-FeO}$ ($\text{MgO} = 3\%$, $\text{FeO} = 55\%$).

The terms γ'_{Me} , p_{CO} , $a_{(\text{MeO})}$, $\gamma_{(\text{MeO})}$ and L_{Me} represent the activity coefficient of Me in the metal melt, the partial pressure of CO gas in the smelting system, the activity of MeO in the slag, the activity coefficient of MeO in the slag, and the partition ratio of metal in the iron slag, respectively. In addition, the terms A_{Me} , B_{Me} , and L_0 are all constants.

In the process of smelting laterite nickel ore to recover Ni, Fe, and Co, the essence of improving metal recovery is to increase the metal distribution ratio (L_{Me}) in iron slag. According to the Equations (3) and (4), increasing furnace temperature is effective in improving the reaction equilibrium constant K_{Me} and accelerating the reaction rate. In addition, it is necessary to reasonably increase the basicity of slag, which is mostly due to (FeO), (NiO), (CoO), and (CaO) all being basic constituents and so the increase of similar oxides in slag can increase $\gamma_{(\text{MeO})}$ oxides in slag.

3.1.2. Optimization of Reasonable Slag Composition

In the smelting process, slag viscosity has a great influence on the diffusion of elements, interfacial chemical reaction, gas escape, heat transfer, loss of nickel and iron elements, and lining life [28–30]. For the smelting process, it is necessary to appropriately reduce slag viscosity to increase liquid fluidity and reduce the mass transfer resistance. Therefore, in this study, slag viscosity is calculated using Factsage software for laterite nickel pre-reduced lumps with different FeO content, basicity, and MgO/SiO_2 ratios and the slag composition was optimized to be suitable for the smelting process.

The degree of reduction of the pre-reduced lumps of laterite nickel ore is an important factor in determining the properties of the slag. In general, with respect to the selective reduction smelting process, the selective reduction of nickel and iron is essentially completed in the pre-reduction of the laterite nickel ore lump and the subsequent smelting process is primarily for slag–iron separation. At the pre-reduction temperature of 1050 °C and the pre-reduction time of 60 min, the reduction roasting of the laterite nickel ore dry lump with a basicity of 0.6 and a natural MgO/SiO_2 ratio is carried out. The metallization rate and FeO content of the pre-reduced lump with different internal coal ratios are shown in Figure 5 while the results of the slag viscosity calculated by Factsage and the melting temperature based on the different FeO content in the pre-reduced lump are shown in Figure 6.

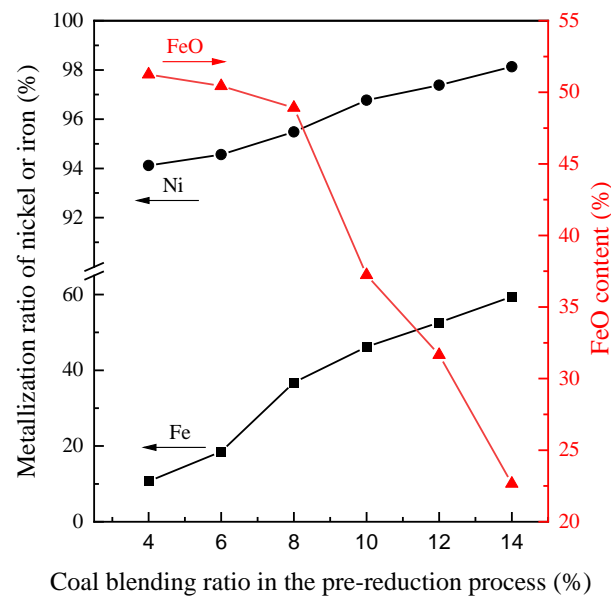


Figure 5. The metallization and FeO content of pre-reduced briquettes with different inner coal ratio/wt.%.

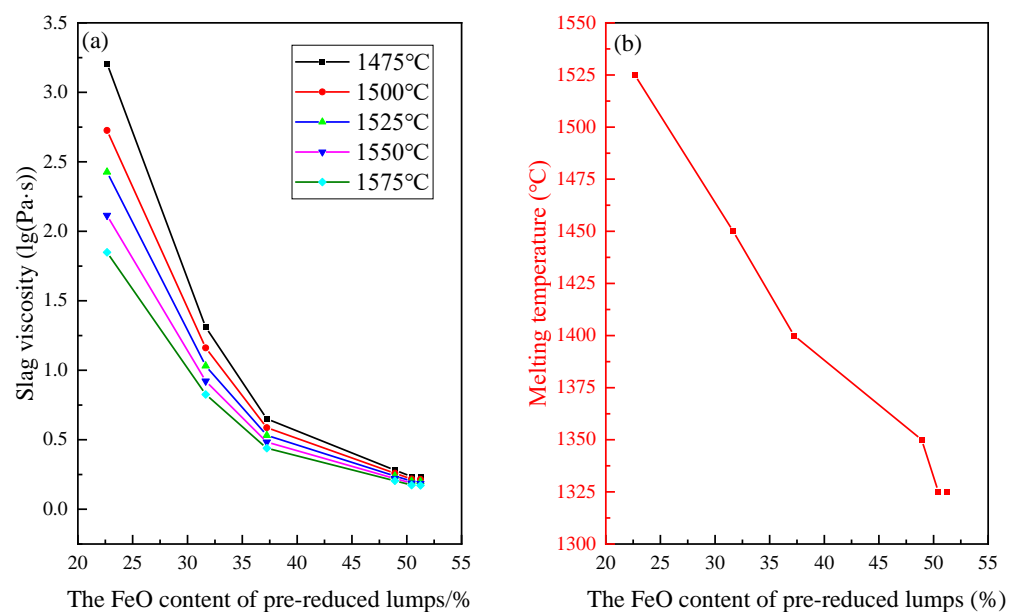


Figure 6. (a,b) Effect of FeO content on the slag viscosity and melting temperature and of furnace burden.

As can be seen in Figure 5, the nickel metallization rate and the iron metallization rate of the pre-reduced lumps both increase significantly as the amount of coal in the pre-reduction process increases and conversely the FeO content decreases significantly. As shown in Figure 6, the results of the thermodynamic calculations show that the melting temperature and the slag viscosity decrease significantly as the FeO content of the pre-reduced lump increases. When the FeO content of the pre-reduced lump is 22.66%, the melting temperature of the slag is 1525 °C, and the slag viscosity under the smelting temperature of 1525 °C is 2.427 lg(Pa·s). As the FeO content of the pre-reduced lump increased to 31.66%, 37.24%, 48.92%, and 50.44%, the melting temperature of the slag was reduced to 1450 °C, 1400 °C, 1350 °C, and 1325 °C, respectively, and the slag viscosity under the smelting temperature of 1525 °C decreases in sequence to 1.032 lg(Pa·s), 0.532 lg(Pa·s), 0.239 lg(Pa·s), and 0.202 lg(Pa·s), respectively. However, when the FeO content of the

pre-reduced lump was further increased to 51.25%, both the melting temperature and viscosity of the slag were reduced even less.

Moreover, increasing the smelting temperature can also significantly reduce the viscosity of the slag. Taking the pre-reduced laterite nickel ore with a FeO content of 50.44% as an example, the slag viscosity is 0.236 lg(Pa·s) when the smelting temperature is 1425 °C. With the smelting temperature increased in sequence to 1450 °C, 1475 °C, 1500 °C, and 1525 °C, the slag viscosity decreased to 0.218 lg(Pa·s), 0.202 lg(Pa·s), 0.188 lg(Pa·s), and 0.174 lg(Pa·s), respectively. The FeO content of the pre-reduced laterite nickel lump should be around 50.44% and the nickel and iron metallization rates of the pre-reduced lump should be 94.56% and 18.53%, respectively, taking into account the melting temperature of the slag.

The change in slag viscosity at 1500 °C with differing basicity and MgO/SiO₂ ratios is shown in Figure 7. The basicity and MgO/SiO₂ ratio of slag are also important factors affecting the slag viscosity. An increase of basicity leads to a substantial increase in slag viscosity. Furthermore, the appropriate increase of MgO/SiO₂ to 0.15–0.3 can effectively reduce the slag viscosity and then slag viscosity is gradually elevated with continuing increase in the amount of MgO/SiO₂.

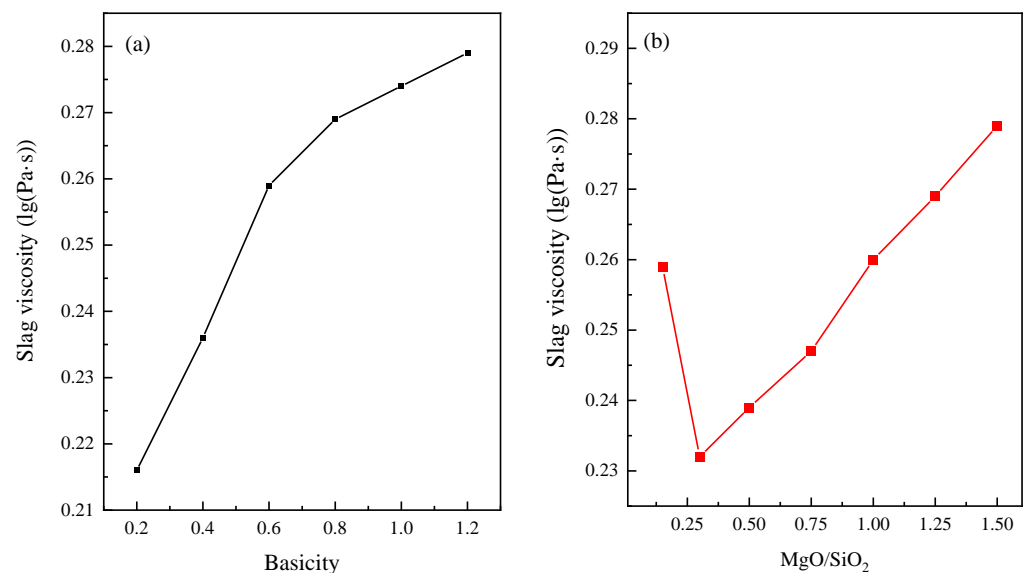


Figure 7. (a,b) Effect of basicity and MgO/SiO₂ ratio on slag viscosity.

3.2. Smelting Process of Pre-Reduced Nickel Laterite

In order to optimize the production parameters, this study systematically explored the impact of smelting parameters such as basicity, FeO content, MgO/SiO₂ ratio, the smelting temperature and the smelting time on the smelting effect during the selective reduction smelting process.

With a fixed MgO/SiO₂ ratio of 0.15, smelting temperature of 1500 °C, and smelting time of 30 min, the influence of basicity on the smelting effect of laterite nickel ore is systematically explored and the results are shown in Figure 8a. It can be seen from this that the iron grade and iron recovery of the ferronickel improved as the grade of the basicity increased while the nickel recovery remained essentially unchanged at more than 96%, but the nickel grades showed a downward trend.

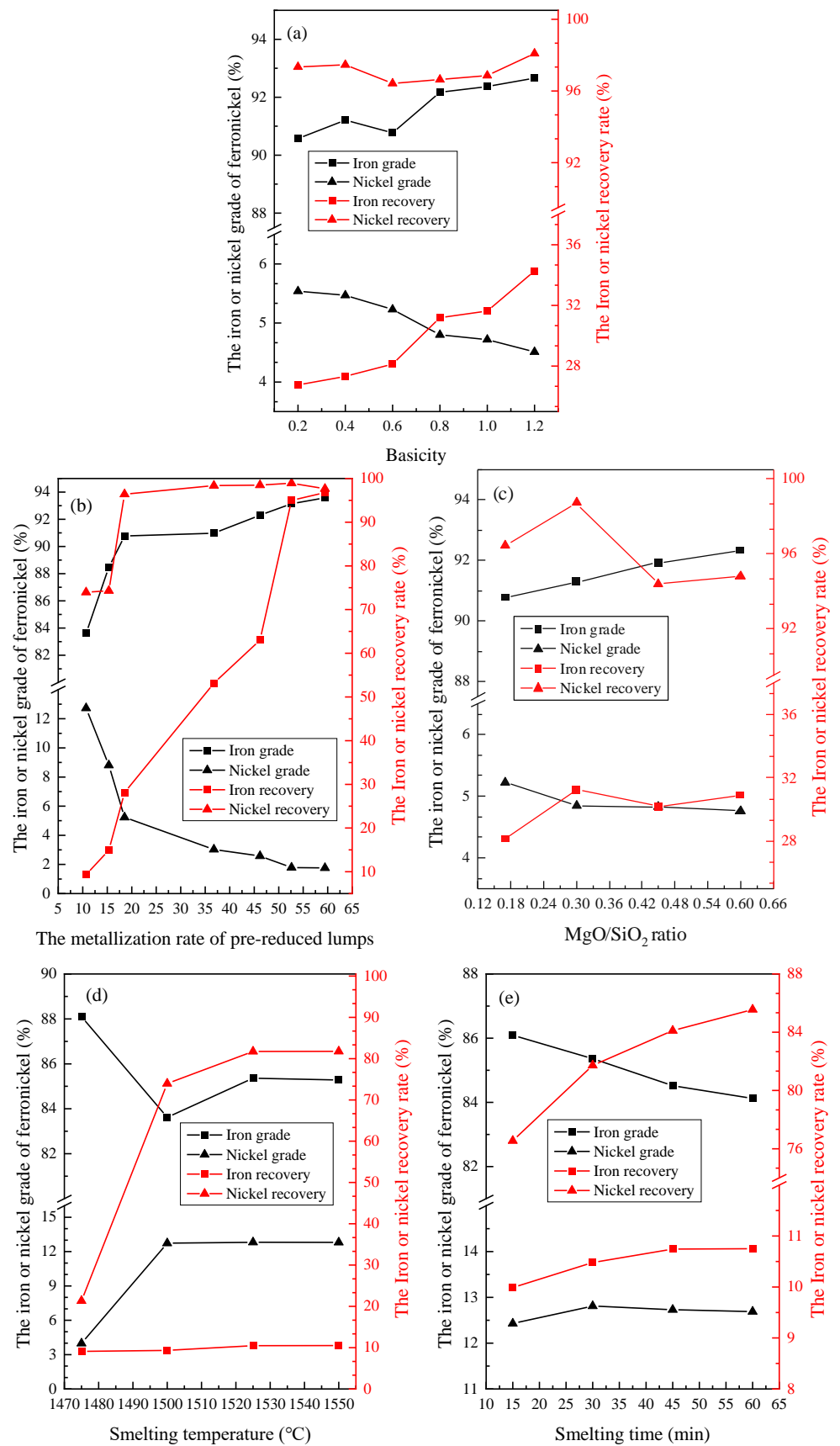


Figure 8. (a–e) Effect of smelting parameters on smelting separation performance.

Under the conditions of a smelting temperature of 1500 °C, smelting time of 30 min, MgO/SiO₂ ratio of 0.15, and basicity of 0.6, the influence of the metallization rate of the pre-reduced lump on the smelting effect of laterite nickel ore is shown in Figure 8b. The nickel grade of ferronickel is only 1.76~3.03% when the iron metallization rate of pre-reduced lumps is 59.44~36.78%. As the metallization rate of the pre-reduced lumps continues to decrease, the iron grade of ferronickel and the iron recovery rate of ferronickel continue to decrease, while the nickel grade gradually increases and the nickel recovery rate decreases. The nickel grade of ferronickel is 5.23% and the nickel recovery rate is 96.42% when the metallization rate of iron contained in the pre-reduced lump iron has a modulation rate of 18.53%. In addition, the nickel grade of ferronickel is as high as 12.73% and the nickel recovery rate is only 73.96% when the iron contained in the pre-reduced lump has a metallization rate of 10.68%. Hence, controlling the iron metallization rate is the key factor in achieving superior ferronickel with a high Ni grade.

Under the conditions of a smelting temperature of 1500 °C, smelting time of 30 min, iron metallization rate of 18.53% and basicity of 0.6, the burdening influence of the MgO/SiO₂ ratio on smelting effect is conducted and the result is shown in Figure 8c. With the increase of the MgO/SiO₂ ratio in the slag, the iron grade and iron recovery have been increased, while the nickel grade and nickel recovery have a downward trend. Therefore, increasing the MgO/SiO₂ ratio can improve the separation effect between slag and alloy, though it does not favor nickel recovery due to the increase of slag viscosity, resulting in greater difficulty of slag and alloy separation.

Using the conditions of an iron metallization rate of 10.68%, nickel metallization rate of 94.12%, basicity of 0.6, MgO/SiO₂ ratio of 0.17, and smelting time of 30 min, this study systematically explored the effect of smelting temperature on the smelting effect of laterite nickel ore. The results are shown in Figure 8d. The effect of the smelting temperature on the recovery of nickel and iron is very obvious. When the melting temperature is 1475 °C, the slag cannot flow freely and the slag and iron are not separated normally while the nickel grade of ferronickel is 3.98% and the nickel recovery rate is only 21.33%. When the smelting temperature increases from 1500 °C to 1575 °C, there is little change in iron grade and iron recovery rate, while nickel grade increases slightly and nickel recovery rate increases from 73.96% to 81.75% with an increase of about 7.8%. This is mainly because the slag viscosity decreases with the increase of smelting temperature, which is conducive to the settlement and fusion of metal particles and the reduction of mechanical inclusion loss of nickel.

When the iron metallization rate of pre-reduced lumps is fixed at 10.68%, the nickel metallization rate is 94.12%, the basicity is 0.6, the MgO/SiO₂ ratio is 0.17 and smelting temperature is 1525 °C during the smelting process, the effect of time on the smelting effect of laterite nickel ore is shown in Figure 8e. The recovery rate of nickel increased from 76.55% to 85.56% as the smelting time increased from 15 min to 60 min. Considering actual production efficiency, the nickel grade is 12.73% and the nickel recovery is 84.11% at a melting time of 45 min. Generally speaking, for the smelting reduction process, prolonging the smelting time can promote the chemical reaction at the slag–iron interface to reach equilibrium, thereby improving the metal recovery rate.

Overall, the suitable parameters for ferronickel smelting of laterite nickel ore during the smelting process are as follows: basicity of 0.60, MgO/SiO₂ ratio of 0.30, nickel metallization rate of 94.30%, iron metallization rate of 10.93%, smelting temperature of 1525 °C, and smelting time of 45 min. The chemical composition of the ferronickel and slag obtained by smelting the laterite nickel ore under the optimal conditions are shown in Tables 3 and 4, respectively. As can be seen from that, the ferronickel has a nickel grade of 12.55% with a nickel recovery of 85.65%, iron grade of 84.61% with the iron recovery of 10.87%, and cobalt grade of 1.36% with a cobalt recovery of 75.92%. To sum up, the product has a high valuable element content and is low in impurities such as S and P contents and the quality of the product is relatively pure. Therefore, after further refining, the ferronickel can be used as a high-quality basis for subsequent stainless steel smelting.

Table 3. Chemical composition of ferronickel/wt.%.

Fe	Ni	Co	Cr	Mn	Si	C	S	P
84.61	12.55	1.36	0.064	0.015	0.032	0.12	0.110	0.003

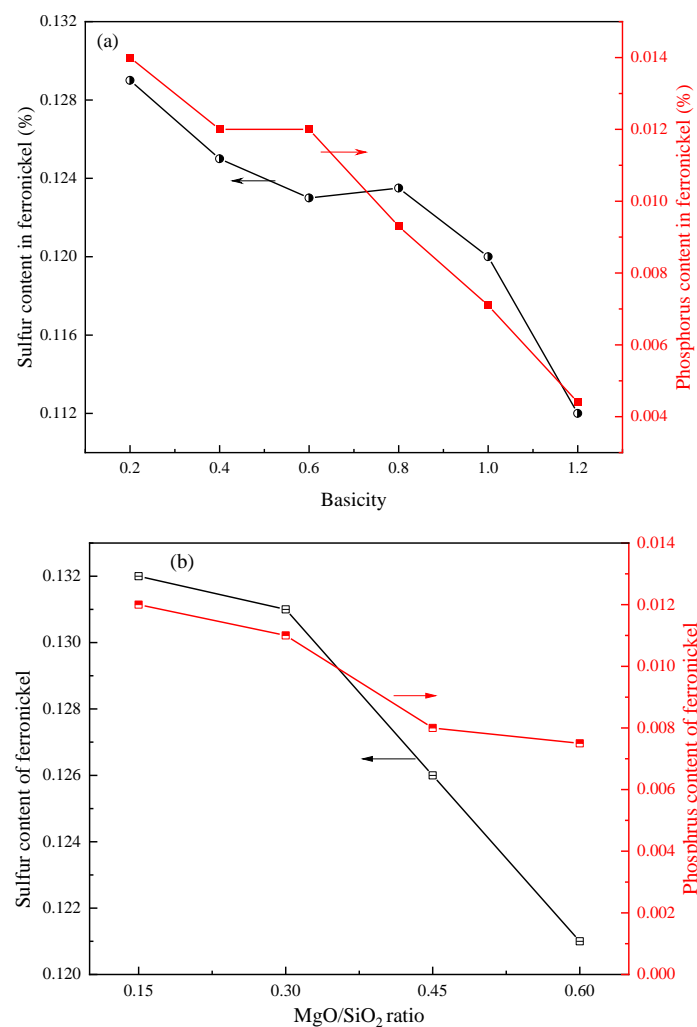
Table 4. Chemical composition of slag/wt.%.

FeO	* MFe	Fe ₃ O ₄	Ni	CaO	MgO	Al ₂ O ₃	SiO ₂	Cr ₂ O ₃	MnO
50.07	2.57	9.28	0.084	5.34	2.69	13.16	8.68	6.22	1.65

* MFe: Magnetic iron.

3.3. Mechanism of Desulfurization and Dephosphorization

Phosphorus and sulfur are harmful elements which can reduce the plasticity, toughness, and welding performance of steel [30]. In the actual stainless steel production process, it is essential to control the content of P and S. In order to improve the quality of ferronickel products, as much phosphorus and sulfur should be removed as possible in the smelting process. Generally, the addition of flux has a significant impact on the removal of phosphorus and sulfur in pyrometallurgy. Therefore, this research systematically explores the effects of basicity and MgO/SiO₂ ratio of slag on the P and S contents of ferronickel product and the results are shown in Figure 9.

**Figure 9.** (a,b) Effect of basicity or MgO/SiO₂ ratio on S and P content in ferronickel.

As shown in Figure 9, with an increase of basicity, CaO content in slag increases, S content in ferronickel decreases from 0.129% to 0.112%, and P content in ferronickel decreases from 0.014% to 0.0044%. Increasing the basicity of slag has a remarkable effect on the removal of S and P. However, the effect of increasing MgO content is significant in dephosphorization, but not in desulphurization. With the MgO/SiO₂ ratio increasing from 0.15 to 0.60, the P content of ferronickel decreased from 0.012% to 0.0072% respectively. Considering the influence of MgO/SiO₂ on slag viscosity and the dephosphorization effect, the recommended ratio of MgO/SiO₂ is 0.2~0.5.

S and P are the main harmful impurities in ferronickel products. The sulphur capacity and phosphorus capacity of slag are important qualitative evaluation indices in evaluating the desulfurization capacity and dephosphorization capacity of slag. This study calculates the phosphorus and sulfur capacity of slag according to the calculation model proposed by Young R W et al. and the specific formulas are shown in Equations (6)–(9) [26–30]. Finally, the effect of basicity and MgO/SiO₂ ratio on the phosphorus and sulfur capacity of slag is investigated and the results are shown in Figures 9 and 10, respectively [26–30].

$$\lg C_s = -13.913 + 42.84\Lambda - 23.82\Lambda^2 - \frac{11710}{T} - 0.02223\omega(\text{SiO}_2) - 0.02275\omega(\text{Al}_2\text{O}_3) \quad (6)$$

where C_s is the sulfide capacity of slag, Λ is optical basicity, $\omega(\text{SiO}_2)$ is the mass fraction of SiO₂ in slag, and $\omega(\text{Al}_2\text{O}_3)$ is mass fraction of Al₂O₃ in slag.

$$\lg C_{\text{PO}_4} = -18.184 + 35.84\Lambda - 23.35\Lambda^2 + \frac{22930\Lambda}{T} - 0.06257\omega(\text{FeO}) - 0.04256\omega(\text{MnO}) + 0.359[\omega(\text{P}_2\text{O}_5)]^{0.3} \quad (7)$$

where C_{PO_4} is the phosphorus capacity of slag, Λ is optical basicity, $\omega(\text{FeO})$ is the mass fraction of FeO in slag, $\omega(\text{MnO})$ is the mass fraction of MnO in slag, and $\omega(\text{P}_2\text{O}_5)$ is the mass fraction of P₂O₅ in slag.

$$\Lambda = \sum_{B=1}^n \chi_B \Lambda_B \quad (8)$$

where Λ is optical basicity and χ_B is the mole fraction of oxide cations, which is also defined as the fraction of each cationic charge neutralizing the negative charge.

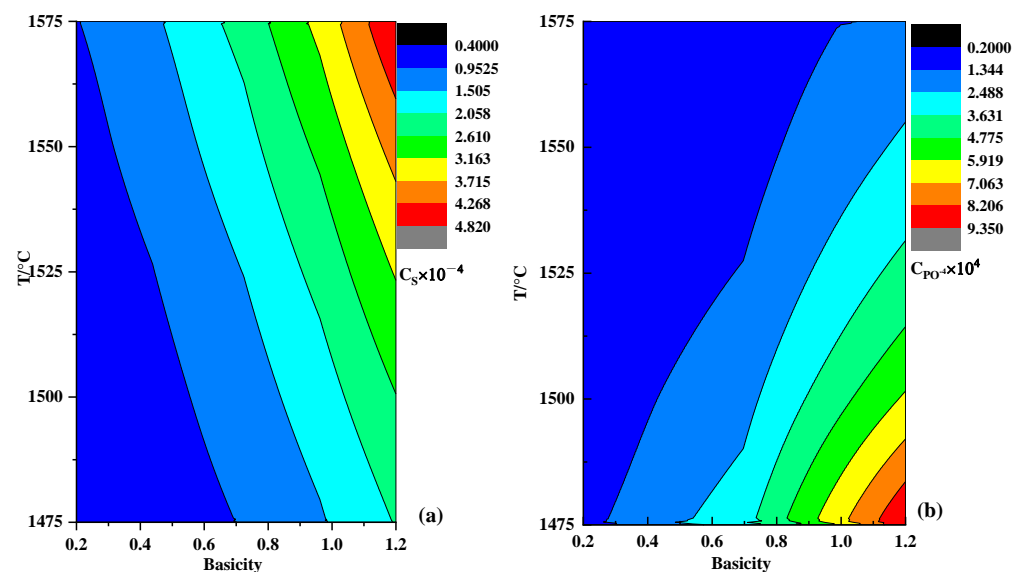


Figure 10. (a,b) Effect of basicity on sulfur and phosphorus capacity of slag.

Therefore, the χ_B can be calculated as follows:

$$\chi_B = \frac{n_0 \chi'_B}{\sum n_0 \chi'_B} \quad (9)$$

where χ'_B is the mole fraction of oxides and n_0 is the quantity of oxygen in each oxide component.

As can be seen, basicity and temperature have a marked impact on phosphorus and sulfur capacity. Increasing basicity helps to elevate sulfur capacity and improve desulfurization capability, resulting in lower S content in the alloy, which also accords with the results shown in Figure 10a. Meanwhile, similar rules can be drawn from Figure 10b. Basicity of slag is beneficial for dephosphorization.

The effect of MgO/SiO₂ ratio on sulfur and phosphorus capacity of slag is presented in Figure 11. As can be seen from the image, the MgO/SiO₂ ratio has a positive effect on the sulfur and phosphorus capacity of the slag, which means the slag with the higher MgO/SiO₂ ratio has a greater ability to hold and remove more sulfide from the metal phase, resulting in an improvement in desulfurization and dephosphorization efficiency and lower S and P content in the ferronickel.

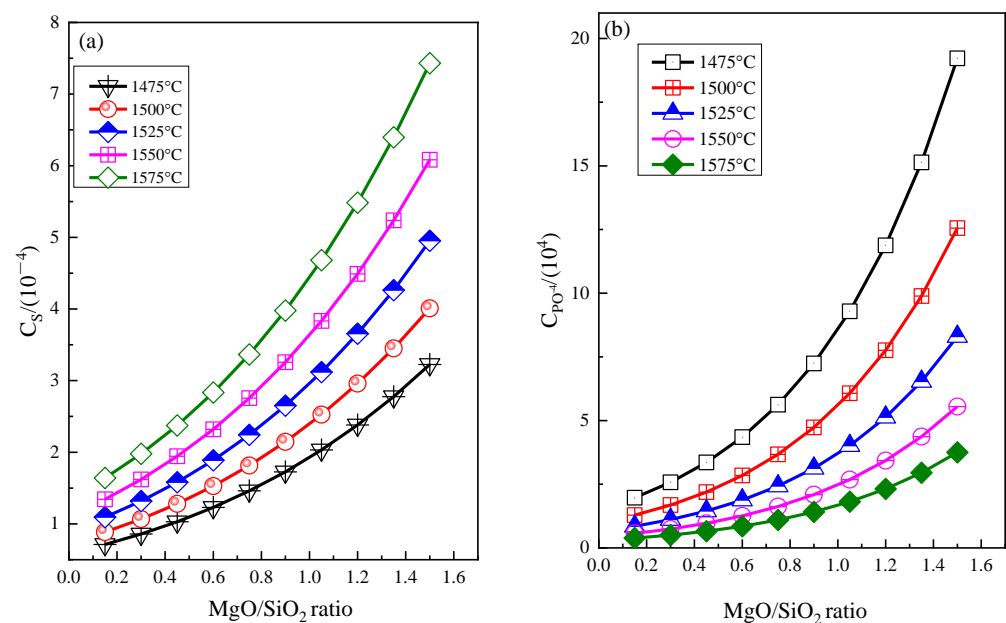


Figure 11. (a,b) Effect of MgO/SiO₂ ratio on sulfur and phosphorus capacity of the slag.

3.4. Implications and Potential Limitations of This Research

Since Indonesia once again restricted exports of laterite in 2022, 90% of China's laterite imports, 50% of which are limonite laterite, come from the Philippines. Chinese stainless steel enterprises are seeking a solution for developing limonite laterite with technological and economic feasibility. In this study, selective reduction smelting technology is introduced in China to smelt limonite laterite, which provides a new alternative method for the production of ferronickel.

After the parameter optimization experiment, ferronickel with nickel and iron grades of 12.55% and 84.61% was obtained from the selective reduction smelting process under the appropriate parameters of an iron metallization rate of 10.93%, nickel metallization rate of 94.30%, basicity of 0.6, MgO/SiO₂ ratio of 0.30, smelting temperature of 1525 °C, and smelting time of 45 min, which is a fine material for the subsequent stainless steel smelting due to its high-grade Ni content and low impurity content.

However, the selective reduction smelting process still has the problem of high smelting temperature due to its imperfection. In the future, further studies on slag type regulation mechanisms and slag phase transition mechanisms will be carried out to find ways to reduce smelting temperature and energy consumption.

4. Conclusions

This paper describes an investigation conducted to upgrade limonite nickel laterite for the preparation of ferronickel by selective reduction smelting technology and the results show that:

- (1) The iron metallization rate of pre-reduced lumps is the most important factor affecting the nickel grade of ferronickel. The nickel grade of ferronickel is only 1.76~3.03% when the metal metallization rate of pre-reduced lumps is 59.44~36.78%. When the iron metallization rate of the pre-reduced lumps is decreased to 10.68%, the nickel grade is increased to 12.73%, but the nickel recovery is reduced to 73.96%.
- (2) Increasing the basicity and MgO/SiO₂ ratio of burden can increase the distribution ratio of Fe and Ni among molten iron and slag and improve the metal recovery rate. At the same time, increasing the content of CaO and MgO in slag can enhance the removal of harmful impurities such as P and S due to the improvement of sulphur capacity and phosphorus capacity of slag. The optimized basicity ratio of MgO/SiO₂ in slag is recommended as 0.5~0.9 and 0.2~0.5, respectively.
- (3) Given a recommended iron metallization rate of 10.93%, nickel metallization rate of 94.30%, basicity of 0.6, MgO/SiO₂ ratio of 0.30, smelting temperature of 1525 °C, and smelting time of 45 min, nickel, iron, and cobalt grades of ferronickel are 12.55%, 84.61%, and 1.36%, respectively. The recovery rates are 85.65%, 10.87%, and 75.92%, respectively. The contents of S and P in ferronickel are 0.11% and 0.0035%, respectively.
- (4) The ferronickel obtained from the selective reduction smelting process is a fine material for subsequent stainless steel smelting due to its high-grade Ni content and low impurity content.

Author Contributions: Investigation, Z.G., C.Y., S.L. and X.W.; resources, D.Z., J.P., Z.G. and T.L.; data curation, and X.W.; writing—original draft preparation, X.W.; writing—review and editing, Z.G. and J.P. All authors have read and agreed to the published version of the manuscript.

Funding: The authors sincerely appreciate the financial support from the National Natural Science Foundation of China (Nos. 52274343 and 52174329).

Data Availability Statement: The data presented in this study are available on request from the corresponding author. The data are not publicly available due to our lab policy or confidentiality agreement.

Conflicts of Interest: The authors declare that they have no known competing financial interest or personal relationships that could have appeared to influence the work reported in this paper.

References

1. Yuan, G.; Ayman, E.; Xi, X. Dynamic analysis of future nickel demand, supply, and associated materials, energy, water, and carbon emissions in China. *Resour. Policy* **2021**, *74*, 102432.
2. Yao, P.; Zhang, X.; Wang, Z.; Long, L.; Han, Y.; Sun, Z.; Wang, J. The role of nickel recycling from nickel-bearing batteries on alleviating demand-supply gap in China's industry of new energy vehicles. *Resour. Conserv. Recycl.* **2021**, *170*, 105612. [[CrossRef](#)]
3. Stainless Steel Council of China Special Steel Enterprises Association. China's Stainless Steel Crude Steel Production in 2021. Available online: http://www.csteelnews.com/xwzx/ylnc/202201/t20220127_59130 (accessed on 1 July 2022).
4. Dalvi, A.; Bacon, W.; Osborne, R. The Past and the Future of Nickel Laterites. In Proceedings of the PDAC 2004 International Convention, Trade Show & Investors Exchange, Toronto, ON, Canada, 7–10 March 2004; The Prospectors and Developers Association of Canada: Toronto, ON, Canada, 2004; pp. 1–27.
5. Mu, W.-N.; Lu, X.-Y.; Cui, F.-H.; Luo, S.-H.; Zhai, Y.-C. Transformation and leaching kinetics of silicon from low-grade nickel laterite ore by pre-roasting and alkaline leaching process. *Trans. Nonferrous Met. Soc. China* **2018**, *28*, 169–176. [[CrossRef](#)]
6. Zhang, J.; Gao, L.; He, Z.; Hou, X.; Zhan, W.; Pang, Q. Separation and recovery of iron and nickel from low-grade laterite nickel ore by microwave carbothermic reduction roasting. *J. Mater. Res. Technol.* **2020**, *9*, 12223–12235. [[CrossRef](#)]
7. Farrokhpay, S.; Filippov, L.; Fornasiero, D. Pre-concentration of nickel in laterite ores using physical separation methods. *Miner. Eng.* **2019**, *141*, 105892. [[CrossRef](#)]
8. Su, C.; Geng, Y.; Zeng, X.; Gao, Z.; Song, X. Uncovering the features of nickel flows in China. *Resour. Conserv. Recycl.* **2023**, *188*, 106702. [[CrossRef](#)]

9. Li, D.; Guo, X. *Fundamental and Technological Study on Treatment of Low-Grade Nickel Laterite by Hydrometallurgical Processes*; Metallurgical Industry Press: Beijing, China, 2015. (In Chinese)
10. Haldar, S. *Platinum-Nickel-Chromium Deposits*; Elsevier: Amsterdam, The Netherlands, 2017. [[CrossRef](#)]
11. Ma, B.; Wang, C.; Yang, W.; Yin, F.; Chen, Y. Screening and reduction roasting of limonitic laterite and ammonia-carbonate leaching of nickel–cobalt to produce a high-grade iron concentrate. *Miner. Eng.* **2013**, *50*, 106–113. [[CrossRef](#)]
12. Zhou, Z.; Ma, B.; Wang, C.; Chen, Y.; Wang, L. Separation and recovery of scandium from high pressure sulfuric acid leach liquor of limonitic laterite. *Process. Saf. Environ. Prot.* **2022**, *165*, 161–172. [[CrossRef](#)]
13. Crundwell, F.K.; Moats, M.; Ramachandran, V.; Robinson, T.G.; Davenport, W.G. *Extractive Metallurgy of Nickel, Cobalt and Platinum Group Metals*; Elsevier: Amsterdam, The Netherlands, 2011. [[CrossRef](#)]
14. Astuti, W.; Nurjaman, F.; Mufakhir, F.R.; Sumardi, S.; Avista, D.; Wanta, K.C.; Petrus, H.T.B.M. A novel method: Nickel and cobalt extraction from citric acid leaching solution of nickel laterite ores using oxalate precipitation. *Miner. Eng.* **2023**, *191*, 107982. [[CrossRef](#)]
15. Ichlas, Z.T.; Jones, S.A.; Ibane, D.C.; Lee, G.-G.; Alorro, R.D. Technospheric mining of scandium from hydrometallurgical tailings of nickel laterite processing: Selection of lixiviant and optimisation of leaching variables. *Miner. Eng.* **2022**, *179*, 107436. [[CrossRef](#)]
16. Kaya, Ş.; Topkaya, Y.A. *Rare Earths Industry, Chapter 11-Extraction Behavior of Scandium from a Refractory Nickel Laterite Ore During the Pressure Acid Leaching Process*; Elsevier: Amsterdam, The Netherlands, 2016.
17. Tu, Y.; Zhang, Y.; Su, Z.; Jiang, T. Mineralization mechanism of limonitic laterite sinter under different fuel dosage: Effect of FeO. *Powder Technol.* **2022**, *398*, 117064. [[CrossRef](#)]
18. Wang, S.; Jiang, Y.; Guo, Y.; Yang, Z.; Chen, F.; Li, G.; Yang, L. Behavior of chromium in the reduction and smelting of high alumina nickel laterite in blast furnace. *J. Mater. Res. Technol.* **2023**, *22*, 2275–2283. [[CrossRef](#)]
19. Shi, Y.; Guo, Z.; Zhu, D.; Pan, J.; Lu, S. Isothermal reduction kinetics and microstructure evolution of various vanadium titanomagnetite pellets in direct reduction. *J. Alloys Compd.* **2023**, *953*, 170126. [[CrossRef](#)]
20. Zhang, Y.; Cui, K.; Wang, J.; Wang, X.; Qie, J.; Xu, Q.; Qi, Y. Effects of direct reduction process on the microstructure and reduction characteristics of carbon-bearing nickel laterite ore pellets. *Powder Technol.* **2020**, *376*, 496–506. [[CrossRef](#)]
21. Guo, Z.; Wang, Y.; Li, S.; Pan, J.; Zhu, D.; Yang, C.; Pan, L.; Tian, H.; Wang, D. Reductive roasting mechanism of copper slag and nickel laterite for Fe-Ni-Cu alloy production. *J. Mater. Res. Technol.* **2020**, *9*, 7602–7614. [[CrossRef](#)]
22. Zhu, D.; Zhou, X.; Luo, Y.; Pan, J.; Bai, B. Reduction Smelting Low Ferronickel from Pre-concentrated Nickel-Iron Ore of Nickel Laterite. *High Temp. Mater. Process.* **2016**, *35*, 1031–1036. [[CrossRef](#)]
23. Hasanbeigi, A.; Arens, M.; Price, L. Alternative emerging ironmaking technologies for energy-efficiency and carbon dioxide emissions reduction: A technical review. *Renew. Sustain. Energy Rev.* **2014**, *33*, 645–658. [[CrossRef](#)]
24. Yu, Y.; Li, B.; Fang, Z.; Wang, C. Energy and exergy analyses of pellet smelting systems of cleaner ferrochrome alloy with multi-energy supply. *J. Clean. Prod.* **2020**, *285*, 124893. [[CrossRef](#)]
25. Liu, P.; Li, B.; Cheung, S.C.; Wu, W. Material and energy flows in rotary kiln-electric furnace smelting of ferro-nickel alloy with energy saving. *Appl. Therm. Eng.* **2016**, *109*, 542–559. [[CrossRef](#)]
26. Guo, Z.; Pan, J.; Zhu, D.; Zhang, F. Green and efficient utilization of waste ferric-oxide desulfurizer to clean waste copper slag by the smelting reduction-sulfurizing process. *J. Clean. Prod.* **2018**, *199*, 891–899. [[CrossRef](#)]
27. Guo, Z.; Zhan, R.; Shi, Y.; Zhu, D.; Pan, J.; Yang, C.; Wang, Y.; Wang, J. Innovative and green utilization of zinc-bearing dust by hydrogen reduction: Re-recovery of zinc and lead, and synergetic preparation of Fe/C micro-electrolysis materials. *Chem. Eng. J.* **2023**, *46*, 141157. [[CrossRef](#)]
28. Huang, X. *Principles of Iron and Steel Metallurgy*, 4th ed.; Metallurgical Industry Press: Beijing, China, 2013.
29. Wang, X. *Iron and Steel Metallurgy*; Metallurgical Industry Press: Beijing, China, 2000.
30. Guo, H. *Metallurgical Physical Chemistry*; Metallurgical Industry Press: Beijing, China, 2004.

Disclaimer/Publisher’s Note: The statements, opinions and data contained in all publications are solely those of the individual author(s) and contributor(s) and not of MDPI and/or the editor(s). MDPI and/or the editor(s) disclaim responsibility for any injury to people or property resulting from any ideas, methods, instructions or products referred to in the content.